PECTORALIS MUSCLE FORCE AND POWER OUTPUT DURING FLIGHT IN THE STARLING

By ANDREW A. BIEWENER

*Department of Organismal Biology and Anatomy, University of Chicago,
1025 East 57th Street, Chicago, IL 60637, USA*

KENNETH P. DIAL

*Division of Biological Sciences, University of Montana, Missoula,
MT 59812, USA*

AND G. E. GOSLOW, JR

*Section of Population Biology, Morphology and Genetics, Division of Biology
and Medicine, Brown University, Providence, RI 02192, USA*

Summary

Force recordings of the pectoralis muscle of European starlings have been made *in vivo* during level flight in a wind tunnel, based on bone strain recordings at the muscle's attachment site on the humerus (deltopectoral crest). This represents the first direct measurement of muscle force during activity in a live animal based on calibrated bone strain recordings. Our force measurements confirm earlier electromyographic data and show that the pectoralis begins to develop force during the final one-third of the upstroke, reaches a maximal level halfway through the downstroke, and sustains force throughout the downstroke. Peak forces generated by the pectoralis during level flight at a speed estimated to be $13.7\,\mathrm{m\,s^{-1}}$ averaged $6.4\,\mathrm{N}$ (28 % of maximal isometric force), generating a mean mass-specific muscle power output of $104\,\mathrm{W\,kg^{-1}}$. Combining our data for the power output of the pectoralis muscle with data for the metabolic power of starlings flying at a similar speed yields an overall flight efficiency of 13 %. The force recordings and length changes of the muscle, based on angular displacements of the humerus, indicate that the pectoralis muscle undergoes a lengthening–shortening contraction sequence during its activation and that, in addition to lift and thrust generation, overcoming wing inertia is probably an important function of this muscle in flapping flight.

Introduction

Studies of animal flight have relied largely upon kinematic data obtained from high-speed light ciné films and measurements of musculoskeletal morphology to estimate the power and mechanical requirements of flight, using models based on

fixed-wing aerodynamic theory (Brown, 1963; Greenewalt, 1975; Lighthill, 1977; Pennycuick, 1968, 1989; Tucker, 1968). These theories predict a 'U'-shaped power curve for level flapping flight, in which the power requirement for hovering flight is high, decreasing to a pronounced minimum at an intermediate speed and increasing thereafter at higher speeds. Metabolic data obtained from birds (Bernstein et al. 1973; Hudson and Bernstein, 1983; Torre-Bueno and LaRochelle, 1978; Tucker, 1972), bats (Carpenter, 1985; Thomas, 1975) and, most recently, bumblebees (Ellington et al. 1990), however, indicate a flatter curve, in which the energy cost of forward flapping flight increases only slightly, if at all, over the range of observed flight speeds. In addition, visualization of the air flow patterns around the wings of birds and bats has shown the importance of unsteady flow and dynamic airfoil shape (Kokshaysky, 1979; Rayner, 1979; Rayner et al. 1986; Spedding, 1987; Spedding et al. 1984), reinforcing the need for empirical data to test models of flapping flight.

Recent skeletal kinematic and neuromuscular studies, based on high-speed cineradiographic films and electromyographic (EMG) recordings of starlings flying in a wind tunnel (Dial et al. 1991; Jenkins et al. 1988), suggest that the pectoralis muscle develops force during the latter half of the upstroke, as it is lengthening, and subsequently shortens to initiate the downstroke. Correspondingly, the supracoracoideus (one of the major upstroke muscles) shows EMG activity during the terminal phase of the downstroke, as it is lengthened prior to the beginning of the upstroke. Because the timing, magnitude and duration of force development can only be inferred from EMG recordings of the muscle, we developed a new approach to measure pectoralis muscle force directly during flight. This approach also enables the first direct calculation of the mechanical power output of an animal during flight. Our measurements confirm that the pectoralis begins to develop force during the upstroke, as the muscle is lengthened, to decelerate the wing, and subsequently shortens to re-accelerate and depress the wing during most of the downstroke.

Materials and methods

Animals and wind tunnel design

Three wild-caught European starlings Sturnus vulgaris (body mass 70–73 g) were trained for 4–6 weeks to fly in a wind tunnel at speeds ranging from 8 to $17\,\mathrm{m\,s^{-1}}$. The birds were encouraged to maintain a steady position in the flight chamber by phototactic stimulation and by placing a group of additional birds in a cage above and in front of the flight chamber. The working section of the wind tunnel has dimensions of 0.914 m (length) × 0.584 m (height) × 0.584 m (width) and is constructed of Plexiglas walls to allow filming of the animal's movements (Fig. 1). The wingspan of the starlings in this study averaged 36.5 cm, leaving 11 cm clearance between the wingtips and the side walls when they flew in the center of the flight chamber. A 17 cm diameter hole located 0.711 m from the front of the flight chamber (78 % of its length) along one wall allows entry of the animal

Side view   Honeycomb
                                                     panel

Fan
and
d.c. motor

0.584   A
         B
0.017

0.711

0.864

0.914   0.470   0.483
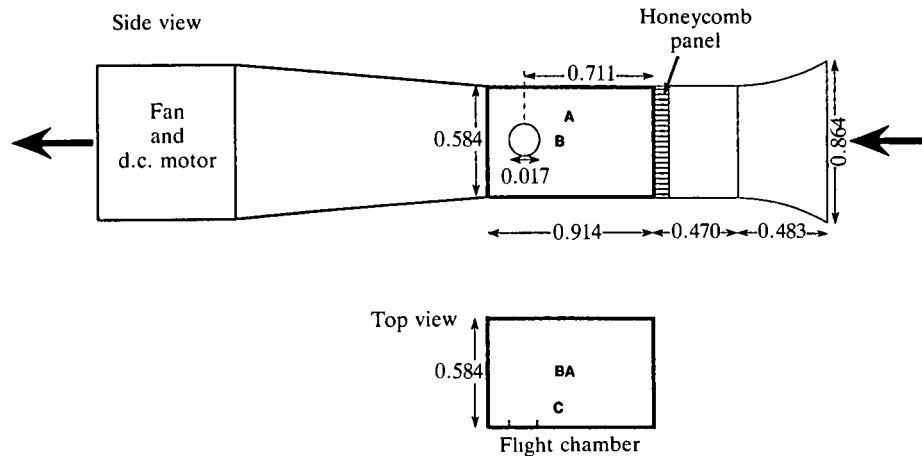
Top view
0.584   BA
             C
Flight chamber

Fig. 1. Diagram of the wind tunnel in side view, showing the dimensions (in meters) of the contraction section, flight chamber and exhaust section of the tunnel. The contraction section has a radius of curvature of 1.04 m. It should be noted that the location of the honeycomb panel just in front of the flight chamber is a poor design feature of the wind tunnel, which not only increases the level of turbulence because of the higher wind speed after the contraction but also generates the turbulence just upstream from the bird. With this design, turbulence levels were 3–5 % in the region where the birds flew (points A and B in side view). Shown below is a top view of the flight chamber indicating the locations of turbulence measurements (A, B and C) with respect to the side port (dash marks). Bold arrows indicate direction of air flow. See text for additional details.

into the flight chamber. This side port was left open during experimental recordings of the animal's flight. Because of the influx of air through this opening, some uncertainty exists concerning the exact flow conditions in the region (center and front half) of the flight chamber where the animals flew (see below). A small 0.95 cm diameter hole in the top of the chamber allows access for a recording cable leading up from the animal's back. Air flow is generated by a d.c. battery-powered fan, located in the exhaust section of the wind tunnel. A d.c. motor was used to minimize electrical interference with recorded signals. Air is drawn in through a contraction section (contraction ratio: 2.19) located at the front of the tunnel, through a 10 cm parallel honeycomb panel (0.63 cm mesh), into the flight chamber and out through the exhaust section of the tunnel. A coarse screen (2.22 cm mesh) located at the rear of the flight chamber isolates the working section of the tunnel. The position of the honecomb panel just in front of the flight chamber is a major deficiency in the design of the wind tunnel that reduces the quality of laminar flow within the flight chamber because of eddies emanating from the downstream end of the jets (a better location to reduce turbulence is at the front of the contraction section). The rather short and, hence, modest contraction section of the tunnel was required to accommodate the space limitations of the X-ray ciné facility at the

Museum of Comparative Zoology (Harvard University), for which the tunnel was originally designed for use in studies of skeletal kinematics during flight (Jenkins *et al.* 1988).

Air speed and turbulence measurements

Wind (flight) speed was originally determined by a pitot anemometer located at the rear of the flight chamber, calibrated using a hand-held Taylor 3100 air speed meter. To correct for the effects of altitude on air density (all experiments were carried out at an altitude of 2100 m in Flagstaff, AZ), measurements of air speed using this device were subsequently corrected by using a Setra Pressure Transducer (sensitivity: $0.7721 \, V \, Pa^{-1}$) and a pitot tube. These latter measurements (and those for turbulence, see below) were made at Brown University, Providence, RI (approximate sea level), with the assistance of Dr S. Karlsson (Professor of Engineering, Brown University). This instrument measures total pressure (dynamic and static), enabling air speed (U, $m \, s^{-1}$) to be calculated based on the following formula:

$$U = 0.7071 Pg\rho_w/\rho_a ,$$

where P is total pressure (Pa) measured by the transducer in volts, g is $9.806 \, m \, s^{-2}$, ρ_w is the density of water ($=1000 \, kg \, m^{-3}$) and ρ_a is the density of air at sea level at $25 \, ^\circ C$ ($=1.186 \, kg \, m^{-3}$). Measurements were made at air speeds of $13.4 \, m \, s^{-1}$ and $10 \, m \, s^{-1}$ in the center of the test chamber (ahead of the side port, where the birds normally flew) and compared to our earlier air speed measurements made with the hand-held Taylor 3100. At both air speeds, the Taylor 3100 measurements were 8–10 % lower than the speeds measured with the Setra pressure transducer. After correcting for this difference and for differences in air density relative to that at sea level, as well as for ambient barometric pressure and temperature (Pennycuick, 1989), we estimate the air speed to be $13.7 \, m \, s^{-1}$ during the conditions of our experiments.

To evaluate the quality of air flow in the flight chamber due to the design limitations of the wind tunnel, turbulence levels were also measured at selected air speeds (7.25, 8.60, 9.67, 11.59 and $12.33 \, m \, s^{-1}$) using a hot-wire anemometer interfaced to a 12-bit A/D converter (± 10 V range) at three locations within the flight chamber (Fig. 1): (A) in the center of the flight chamber slightly above the side port with the door open, (B) 12 cm in front of the side port, center of chamber (the normal flight position of the birds), and (C) 10 cm from the side wall (15 cm off-center), 12 cm in front of the port. Turbulence was also measured at these three locations with the side port closed. Samples were obtained at 1 kHz for a period of 16 s. Using a fast Fourier transform, a spectral analysis of the digitized waveforms was then carried out. Turbulence levels (defined as the root mean square of U in the direction of flow) in the center of the flight chamber with the side port open were $0.334 \, m \, s^{-1}$ and $0.462 \, m \, s^{-1}$ at the respective air speeds of $9.67 \, m \, s^{-1}$ and $12.33 \, m \, s^{-1}$. Overall, turbulence levels of 3–5 % were measured at the different locations in the wind tunnel with the port open. Spectral analysis

showed that most of the power was contained in frequencies less than 10 Hz, which is to be expected for a tunnel of this design. Despite the deficiencies of our present wind tunnel design, this level of turbulence is similar to that reported in other wind tunnels that have been used to study freely flying animals (range 1–7 %, Hudson and Bernstein, 1983; Rothe and Nachtigall, 1987; Thomas, 1975; Torre-Bueno and LaRochelle, 1978; Tucker and Parrott, 1970). Closing the side port had the effect of slightly increasing turbulence and air speed. Although major shifts in air flow direction and speed in the region in which the birds flew due to the influx of air through the side port cannot be ruled out, the possibility that this was a serious problem in the present experiments seems low as the animals were always observed to maintain a consistent forward orientation (parallel to the side walls) when flying. In general, we consider the 5 % level of turbulence in the present wind tunnel design to be of minimal concern in the context of the measurements of muscle force reported here.

Surgery and in vivo *pectoralis force measurement*

After training, the force developed by the pectoralis muscle (pars thoracicus) during flight was determined by making *in vivo* strain recordings from the dorsal surface of the deltopectoral crest (DPC) of the humerus, underneath which the pectoralis inserts (Fig. 2). In effect, this approach uses the DPC as a 'force transducer' to monitor muscle tension dynamically within the animal during flight.
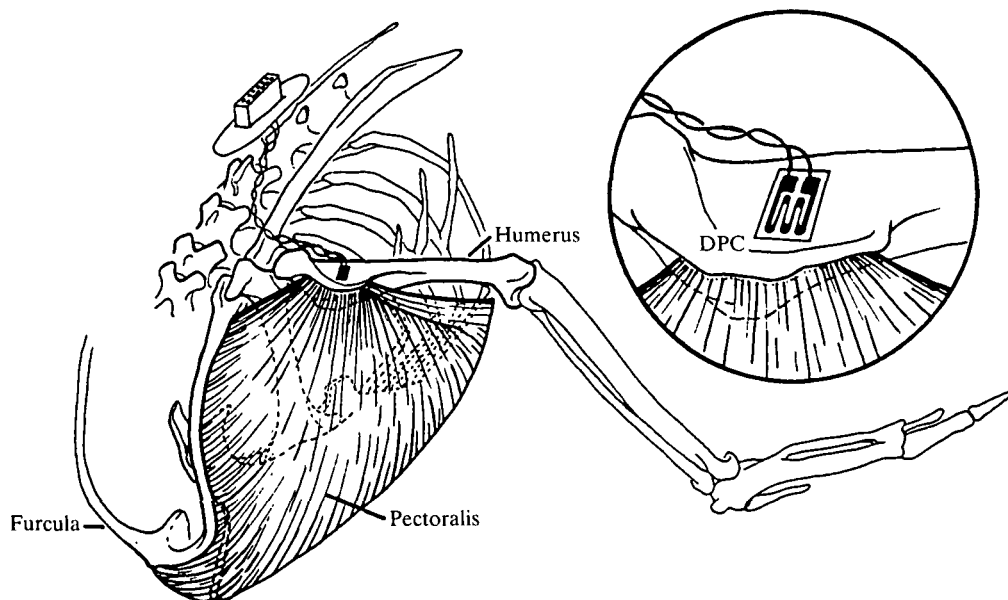

Fig. 2. An oblique antero-dorsal view of the shoulder of the starling with the shoulder skeleton exposed, showing the position of the strain gauge (dark rectangle) attached to the dorsal surface of the deltopectoral crest (DPC) of the humerus. The pectoralis (both sternal and thoracic portions of p. major, shaded) attaches *via* a short tendinous insertion on the ventral surface of the DPC.

The approach requires that temporal changes in DPC strain faithfully track changes in pectoralis muscle tension applied to the DPC; that is, the DPC must function as a stiff spring. This is an important consideration, given the high wing-beat frequencies (generally in the range 12–17 Hz) used by the starling during flight, as most biological materials, including bone, exhibit some viscoelasticity (the strain gauge itself has no limiting frequency response). Over a range of frequency from 0.1 to 100 Hz, however, Lakes et al. (1979) found that the dynamic loss tangent of human and bovine bone samples subjected to dynamically varying torsional and biaxial loads decreases from 0.025 to 0.009. The loss tangent is a measure of the amount of energy dissipated by viscous interactions within the material. These values indicate a phase lag of about 0.017 rad. Assuming that the material properties of the bone in the starling DPC are similar to those in the cortex of human and cow bone, this indicates very little time hysteresis (about 0.4 ms at a frequency of 15 Hz) between applied force to the DPC and resulting (measured) strain. Consequently, it seems reasonable to believe that the temporal patterns of DPC strain we measure correspond well to changes in applied force within the range of frequencies at which the starlings fly. An additional concern, however, is the possibility that changes in humeral and pectoralis orientation/recruitment patterns during the wing-beat cycle might alter the relationship between applied tension and DPC strain measured by the strain gauge (see below).

To make the bone strain recordings, the birds were anesthetized (ketamine 25 mg kg^{-1} and xylazine 25 mg kg^{-1}, supplemented as needed) and the feathers removed over the left shoulder, over the back between the wings and along the ventral aspect of the pectoralis near its origin from the keel of the sternum. The dorsal surface of the deltopectoral crest was exposed for attachment of the strain gauge by making a small incision through the skin and reflecting the deltoid muscle's insertion from the anterior border of the DPC (this procedure had no discernible effect on the subsequent flight performance of the bird). The surface of the DPC was lightly scraped with a periosteal elevator, defatted with methylethylketone and allowed to dry thoroughly before bonding a single-element metal foil strain gauge (type FLE-1, Tokyo Sokki Kenkyujo) to the bone's surface with a rapid, self-catalyzing cyanoacrylate adhesive. To maximize sensitivity of the strain gauge to strains produced by tension in the pectoralis and to minimize sensitivity to strains transmitted through the shaft of the bone, we attached the strain gauge orthogonal to the bone's longitudinal axis. Tension exerted by the pectoralis muscle bends the DPC (which forms a short 'cantilever' projecting anteriorly from the proximal shaft of the humerus) by pulling on it ventrally to produce a primary axis of tensile strain orthogonal to the longitudinal axis of the bone. In contrast, the principal axis of strain within the midshaft of most long bones is aligned close to the longitudinal axis of the bone (Biewener and Taylor, 1986; Biewener et al. 1988b; Rubin and Lanyon, 1982). Strains recorded from the DPC gauge during hand manipulation, to simulate bending, torsion and compression associated with aerodynamic and inertial loading of the whole bone, were only 5.1±0.8 % (N=15)

of the strain levels recorded during flight. As the ventral surface of the DPC is the exclusive site of attachment of the pectoralis (the primary wing depressor in birds) and is relatively isolated from strains produced by adjacent muscle attachments, the DPC represents an ideal skeletal structure for transducing muscle force from localized bone strain.

The lead wires from the strain gauge (36 gauge, Teflon) were passed underneath the deltoid muscle, over the shoulder and subcutaneously to a connector mounted on the animal's back, between the wings. The connector was secured by suturing it to ligaments and fascia attaching to the spines of thoracic vertebrae. The skin was sutured tight about the connector and sealed with a silicone rubber adhesive (Dow Corning). In addition to the strain gauge, a bipolar hook EMG electrode constructed of 0.1 mm enamel-insulated silver wire (California Fine Wire), with 0.5 mm tip exposure and 0.5 mm inter-tip distance, was implanted in the pectoralis near to its origin from the sternum using a 25 gauge hypodermic needle. The EMG leads were sutured to connective tissue along the keel of the sternum (to maintain slack in the wire) and passed subcutaneously to the connector on the animal's back. All skin incisions were sutured closed.

Bone strain and EMG recordings

After a 24 h recovery period, recordings of *in vivo* DPC strain, pectoralis EMG and high-speed light film (HI-CAM, Redlake, Inc.) were made of the animals during flight at $13.7 \, \text{m s}^{-1}$. Because the birds flew sporadically at speeds much lower or higher than this, we report data at this speed only. For most animals, recordings were made over a 2-day period. DPC strain was amplified *via* a Wheatstone bridge circuit (Vishay model 2120, Micromeasurements) and recorded on FM tape (Hewlet-Packard, model 3694A), together with the EMG signal and a synchronization pulse from the camera's shutter. The EMG signal was band-pass filtered at 30 and 3000 Hz (Grass P511 preamplifier), with a 60 Hz notch filter, and amplified 500 times. Analog output of the DPC strain and EMG signals from the FM tape recorder for certain flight and calibration sequences were digitally sampled at 2040 Hz (Kiethley DAS) and entered into an IBM-AT computer for calibration of pectoralis force from DPC strain (see below) and to establish the timing of the pectoralis EMG in relation to pectoralis force generation.

Force calibration

Following the flight recordings, bone strain measurements were calibrated to muscle force *in situ* by tetanic nerve stimulation of the pectoralis muscle and by direct tension applied by pulling *via* a silk suture tied about muscle's tendinous insertion to the DPC. For tetanic stimulation, the birds were deeply anesthetized with ketamine ($25 \, \text{mg kg}^{-1}$) and xylazine ($25 \, \text{mg kg}^{-1}$) before exposing the rostral and caudal pectoral nerves. Silver bipolar electrodes were attached to the nerves and isolated by sheathing the nerves and electrodes in 10 mm lengths of silastic tubing (0.5 mm i.d., Dow Corning). The humerus was left intact at the shoulder in

an attempt to simulate mechanical loading of the DPC during flight. A short length of silk suture (compliance: $0.045\,\mu m\,N^{-1}cm^{-1}$) was tied around the distal end of the humerus and connected to an isometric force transducer (Grass, model FT10). The bird was stabilized in a circulating bath ($39\,^\circ C$) by clamps on the keel of the sternum, the coracoid and the spines of thoracic vertebrae.

Measurements were made with the humerus held in three positions (0°, 45° and 75° elevated; protracted 60° from the sagittal plane of the shoulder) to test for the possibility that differences in the direction of muscle pull during the wing stroke produced differing strains in the DPC. This covers most of the normal range of positions of the humerus during steady level flight when the pectoralis is active (75° above horizontal to 23° below horizontal; Jenkins et al. 1988; Dial et al. 1991). At each orientation, the pectoralis was supramaximally stimulated ($0.1\,ms$ pulse duration) at $100\,Hz$ for a total duration of $1\,s$, and tetanic force, together with the voltage output of the strain gauge, was recorded (Fig. 3A). Force exerted by the
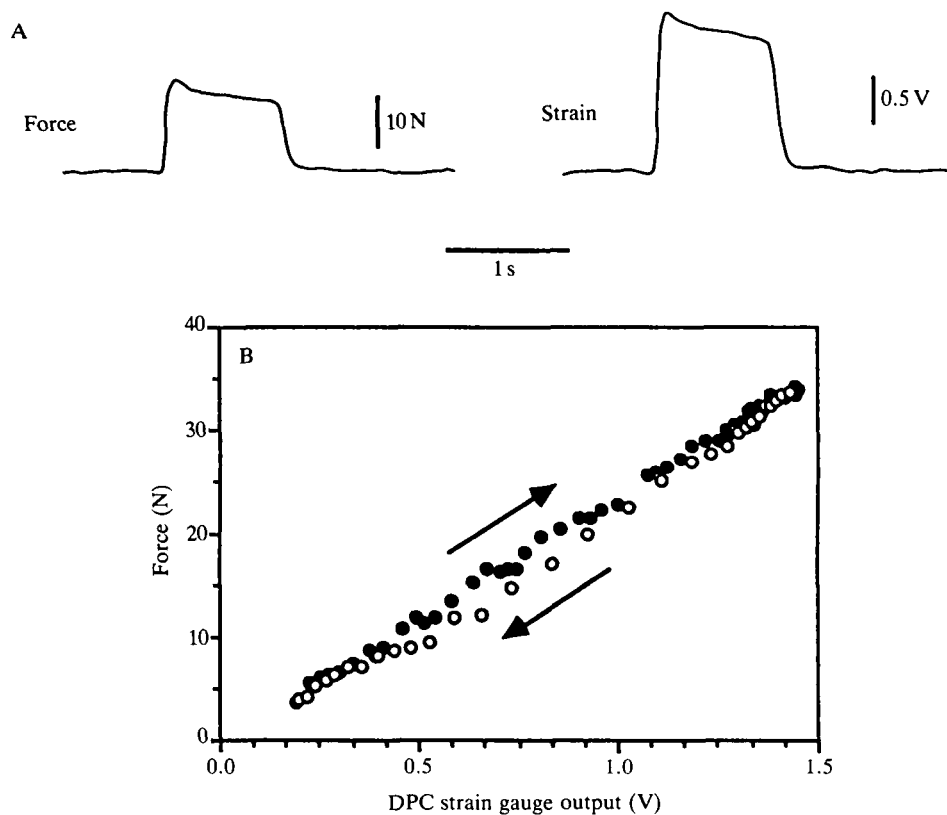

Fig. 3. Strain gauge force calibration. (A) Isometric tetanic force measured from the pectoralis muscle and the corresponding strain recorded from the deltopectoral crest during a 1 s tetanus. (B) Representative calibration curve for the rise (●) and fall (○) in tetanic muscle force vs DPC strain output.

muscle was calculated by accounting for the difference in moment arms about the shoulder. Measurements made at 45° and 75° elevation were averaged to determine the maximal *in situ* isometric force of the muscle (forces measured at 0° were generally 25–30 % lower).

In general, linear calibrations of muscle force were obtained over the range of bone strain recorded at the DPC during flight. Both the magnitude and time course of force development were well represented by the strain recorded from the gauge (Fig. 3A). Calibrations of the DPC strain gauge by direct pulls were also carried out over the same range of orientations as during isometric stimulation of the muscle.

The voltage outputs of the DPC strain gauge and isometric force transducer were digitally sampled during the rise and fall in force and fitted to a reduced major axis (model II) regression to obtain a dynamic calibration of the strain gauge's response to a rise and fall in force (Fig. 3B). In all cases, we obtained excellent linear fit of the data, with correlation coefficients that exceeded 0.90 (mean 0.98 ± 0.03, $N=35$) and 95 % confidence intervals that were less than 5 % of the calibration slope. In general, some hysteresis was noted. For all calibrations carried out on all birds, the slope of the rise in force differed by 11 ± 5 % from the slope of the fall in force. The average of these slopes was used to establish the calibration of strain voltage output to force. Overall differences in calibration among the three animals were 17 ± 8 % as a result differences in orientation of the humerus and 15 ± 7 % as a result of the method of tension development (tetanus *versus* direct pull); ranging from 5.23 to $6.21\,\mathrm{N\,V^{-1}}$ for the three animals. An average value for the calibration of each strain gauge was used to convert strain voltage output to force for each animal during flight.

Muscle fiber area measurements

The pectoralis muscle of starlings has a pinnate fiber architecture that is organized in two differing planes (Dial *et al.* 1991). Muscle fibers are angled with respect to a central fascial sheet (which condenses to form the muscle's tendinous insertion), both in relation to their site of origin from the ribs and the sternum (as seen at the muscle's superficial surface) and to their depth within the muscle as they arise from the keel of the sternum. Because of this complex fiber architecture, measurements of muscle fiber length and fiber angle (with respect to the orientation of the central tendinous sheath and the muscle's presumed line of action) were made at regular intervals about the muscle at both its outer ($N=9$) and deep ($N=7$) surfaces. Typical measurements for one muscle showed muscle fiber lengths ranging from 19.2 to 35.2 mm (mean 27 ± 6.1 mm) and pinnation angles ranging from 8 to 25° (mean $14\pm4.8°$). Mean fiber length and pinnation angle, together with the muscle's mass, were used to calculate the muscle's fiber cross-sectional area according to the method of Alexander (1977), assuming a density of $1060\,\mathrm{kg\,m^{-3}}$ for vertebrate striated muscle. It is important to note that this calculation includes non-contractile components of the muscle (e.g. mitochondria and capillaries) and, hence, overestimates the force-generating component of

the muscle's fiber area. Calculations of muscle fiber cross-sectional area were used to estimate average overall muscle stress based on our measurements of *in vivo* muscle force.

Results and discussion

Timing of pectoralis force and EMG

When flying at a speed estimated to be $13.7\,\mathrm{m\,s^{-1}}$, the starlings beat their wings at a mean frequency of $15.0\pm0.7\,\mathrm{Hz}$, corresponding to a wing-beat cycle of $67\pm3\,\mathrm{ms}$. The wing-beat cycle can be divided into an upstroke phase lasting 31 ms (46 % of stroke period) and a downstroke phase lasting 36 ms (54 % of stroke period). During level flight, the pectoralis begins to develop force during the final one-third of the upstroke, $3.1\pm0.4\,\mathrm{ms}$ ($N=37$) after the onset of EMG activity, when the humerus is elevated 45–50° above horizontal (Figs 4 and 5). As muscle force increases, the wing continues to elevate (to 75° above horizontal), which presumably actively lengthens the pectoralis muscle fibers, as little in-series tendon exists between the muscle fibers and their insertion on the DPC. This active lengthening does negative work to decelerate the wing and initiate the downstroke. Muscle force typically peaks $19\pm6\,\mathrm{ms}$ ($N=37$) after the upstroke–downstroke transition. Although EMG activity of the pectoralis lasts only $27\pm2\,\mathrm{ms}$, the duration of muscle force is $44\pm3\,\mathrm{ms}$ (66 % of the wing-beat period), lasting throughout nearly the entire downstroke (Fig. 5). Thus, after initially being lengthened, the pectoralis subsequently shortens, performing positive work to accelerate the wing downward. This timing of muscle force development indicates that, in addition to generating lift and thrust during the downstroke, a major function of the pectoralis is to counter the inertia of the wing as it makes the transition between the upstroke and downstroke.

Given the extremely low loss modulus of bone when subjected to dynamic loading (Lakes *et al.* 1979), the effect of hysteresis on our estimates of both the time course and magnitude of force developed by the pectoralis is likely to be negligible even at a wing-beat frequency of 15 Hz. Over the time period of force development of the pectoralis (30 ms or 45 % of the wing-beat period), the delay between applied pectoralis force and measured DPC strain is probably less than 0.2 ms. For an average rate of force increase by the pectoralis of $203\,\mathrm{N\,s^{-1}}$, this indicates a potential error of $0.04\,\mathrm{N}$ ($<1\,\%$) in our measurement of peak force.

EMG activity in the supracoracoideus muscle (the primary wing elevator) commences $39\pm1\,\mathrm{ms}$ ($N=20$) after that of the pectoralis EMG at this flight speed, near the end of the downstroke (Dial *et al.* 1991). Given that both muscles have a similar electromechanical delay (time from onset of EMG to onset of force development), these data suggest that the supracoracoideus begins to develop force about 5 ms prior to the decline to zero force in the pectoralis. Our recordings show that the pectoralis still exerts $1.3\pm0.3\,\mathrm{N}$ of force at this time (Figs 4 and 5), indicating antagonistic activity between these two muscles. However, this suggestion must be treated with some caution, given the uncertainty of establishing a zero
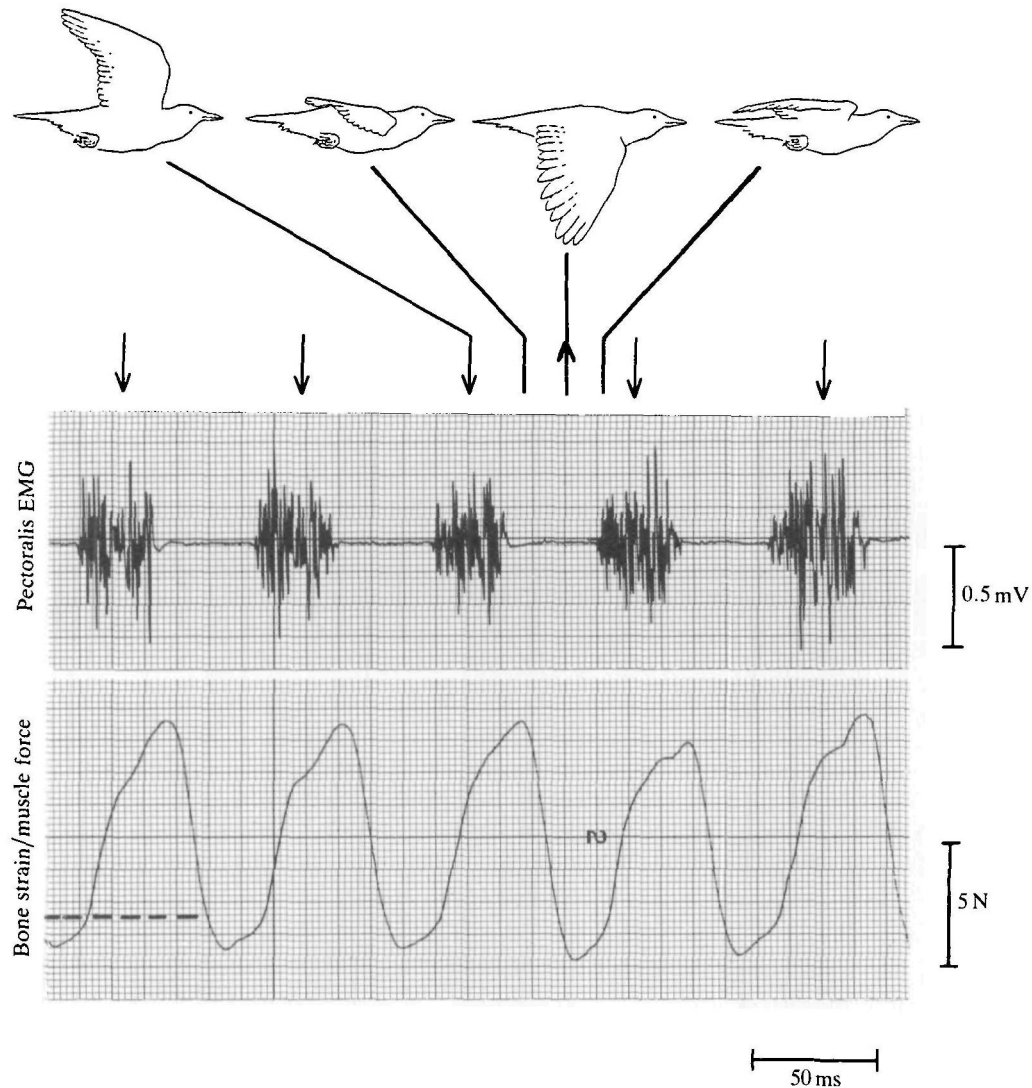
Fig. 4. Representative pectoralis EMG and bone strain/muscle force recordings for five wing-beat cycles during steady level flight at 13.7 m s^{-1} in relation to the kinematics of the wing-beat cycle shown above (downward arrows denote the start of successive downstrokes and the upward arrow denotes the start of an upstroke). The dashed line denotes zero tension in the pectoralis, which was determined when the bird landed and rested following a period of flight. The decrease in voltage (or strain) output below this level during flight probably reflects changes in the direction of muscle pull (which is most extreme at the end of the downstroke) and activation of the supracoracoideus, which has a tendinous insertion on the most proximal, anterior border of the deltopectoral crest. This leads to some uncertainty in the precise timing of zero force in the pectoralis.
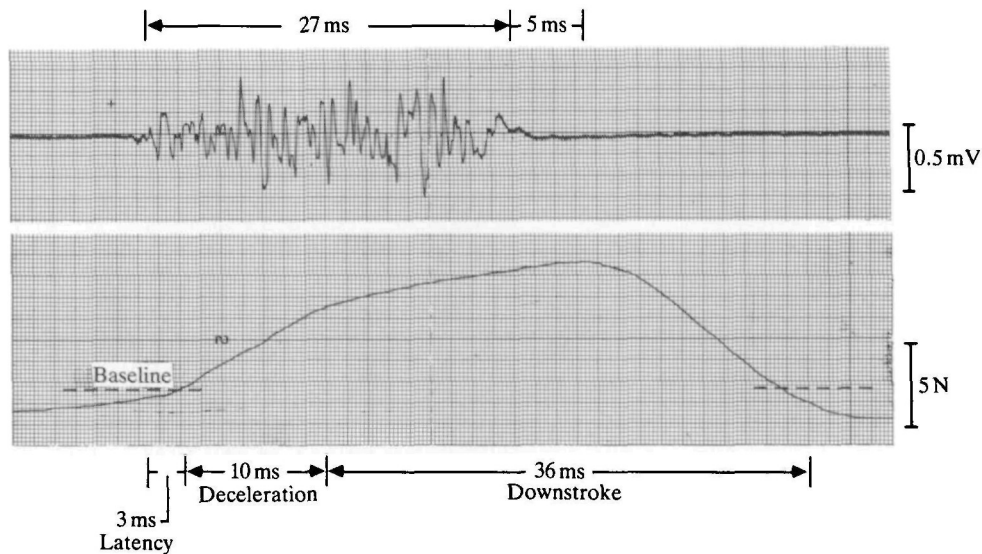
Fig. 5. Expanded recording of pectoralis EMG and muscle force for a single wing-beat cycle (the third cycle shown in Fig. 4), showing that the pectoralis develops force during the latter one-third of the upstroke (wing deceleration), when the humerus is elevated 45° to the horizontal. The latency of force relative to the onset of its EMG is 3 ms. The rate of force development (slope) decreases slightly as the wing reverses direction and begins the downstroke. Maximal force is achieved 19 ms after the upstroke–downstroke transition and 5 ms after cessation of EMG activity. The duration of muscle force (44 ms) exceeds the duration of its EMG (27 ms), lasting throughout nearly the entire downstroke. The wing-beat period was 67 ms.

force level from the DPC strain recordings because of the effect of differences in the direction of muscle pull in relation to the orientation of the humerus on the force calibration of the strain gauge (particularly at the extremes of the bone's range of motion). If the timing of EMG relative to *in vivo* force development in the supracoracoideus parallels that of the pectoralis, it seems likely that the supracoracoideus muscle also undergoes a lengthening–shortening contraction sequence to counter wing inertia at the end of the downstroke.

Pectoralis force, length change and power output

The force developed by the pectoralis muscle in relation to changes in fiber (fascicle) length for one contraction cycle is shown in Fig. 6. The average length change of the muscle's most superficial fibers was calculated based on skeletal kinematic data (Dial *et al.* 1991). The muscle's mean unloaded (resting) fiber length is 34 mm (at its superficial surface, where changes in fiber length are calculated). Angular excursion of the humerus under these conditions of flight is nearly 100° (ranging from 75° above to 23° below horizontal; the humerus is protracted only slightly during the downstroke). Because the pectoralis has a very

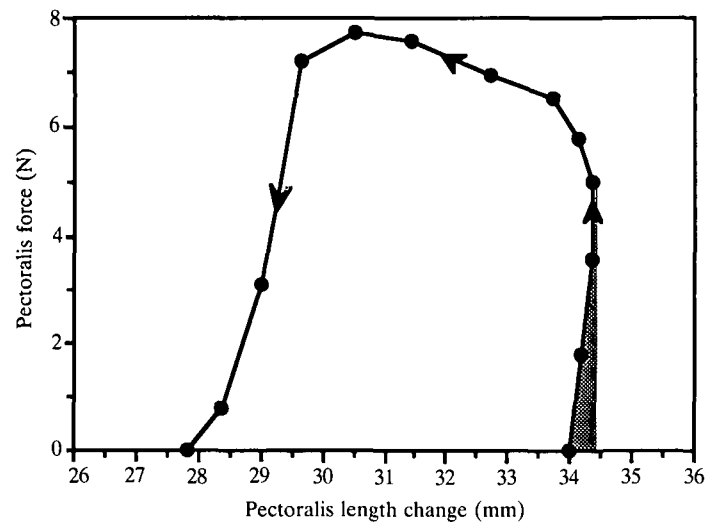Fig. 6. Force developed by the pectoralis of a starling flying at $13.7\,\mathrm{m\,s^{-1}}$ plotted against changes in pectoralis fiber length for one contraction cycle. Individual points represent values of muscle length change determined from skeletal kinematics of the humerus, shoulder and sternum of the starling (Dial *et al.* 1991) at twelve equal time increments, normalized as a fraction of the contraction cycle and correlated with values of force determined at corresponding time intervals. Resting (unloaded) length is assumed to be 34 mm, the average length of the most superficial layer of pectoralis muscle fibers. The shaded region indicates negative work performed by the muscle when it is stretched by the wing's inertia during the final one-third of the upstroke. The unshaded region represents the net positive work performed by the muscle in one contraction cycle. Overall shortening of the muscle corresponds to a fiber strain of 0.20. Arrowheads show the direction of force development relative to length change.

short tendinous insertion on the DPC of the humerus, the series elasticity (stretch) of its tendon is presumably quite small. Consequently, length changes that we calculate from angular displacements of the humerus are probably very close to those of the muscle fibers. Given that the pectoralis has a mechanical advantage of 5.2 mm at the shoulder (mean for all three birds) and based on changes in the orientation of these fibers from the keel of the sternum to the deltopectoral crest, the angular displacements of the humerus during level flight correspond to an average active stretching of the outermost layer of muscle fibers of about 0.5 mm during the upstroke and an overall active shortening of 6.8 mm during the downstroke. Hence, these fibers stretch 1.5 % and shorten 20 % of their resting length. The area under the curve shown in Fig. 6 represents the work done by the muscle during different phases of its contraction (assuming that all muscle fibers shorten by an equal fraction of their length). The shaded region indicates the negative work (1.0 mJ) absorbed by the muscle as it is stretched to decelerate the wing. The total area under the curve (shaded plus unshaded) represents the

Table 1. *Morphological and* in vivo *force data for three European starlings* (Sturnus vulgaris) *flying at 13.7 m s^{-1} (level flight)*

| Animal | Body mass (g) | Pectoralis | | | Pectoralis force (N)† | N | % Maximum isometric force‡ |
		Mass (g)	Area (mm^2)	Corrected area* (mm^2)			
A	73	5.42	197	118	6.48±0.52	52	28.3
B	72	5.46	172	103	7.76±1.17	39	33.9
C	70	5.27	191	115	5.18±0.46	47	22.6

* Based on a combined mitochondrial and capillary volume density of 40 % in the pectoralis; see text for details.

† Mean values±s.e.

‡ Calculated based on a value of 22.9 N for maximum isometric force (average for measurements of *in situ* isometric force made with the humerus elevated at 45° and 80° above horizontal).

positive work (37.4 mJ) performed by the muscle as it subsequently shortens during the downstroke.

As the pectoralis generates nearly all of the lift and thrust required for flight in birds, we can obtain a direct estimate of the total mean power output of the whole animal during flight by multiplying these measurements of muscle work (for both muscles) by the animal's wing-beat frequency: $0.0374\,J \times 2 \times 15.0\,Hz = 1.123\,W$. Although this value underestimates the animal's total mean power output, by neglecting work performed by the supracoracoideus and deltoideus during the upstroke, as well as by other forelimb muscles, this underestimate is unlikely to be very large and is offset by the additional power required to overcome drag associated with the EMG and strain gauge lead wires trailing from the animal. Mean power output of the pectoralis muscle, therefore, averages 104 W kg^{-1} (total pectoralis muscle mass=0.0108 kg, Table 1) during level flight at a speed near 13.7 m s^{-1}.

At the moderately fast flight speeds studied here (starlings can achieve speeds of 18 m s^{-1} or higher; Torre-Bueno and LaRochelle, 1978), the pectoralis muscle develops 6.4±1.4 N of force (average for all three birds; Table 1). In two of the birds for which we obtained reliable *in situ* data, maximal isometric force of the starling pectoralis averaged 22.9±6.2 N (for elevations of the humerus at 45° and 75°; Fig. 3). The forces developed by the pectoralis during steady level flight at this speed, therefore, average 28 % of maximal isometric force. Based on our anatomical measurements of pectoralis fiber cross-sectional area (mean: 187 mm^2) and isometric force, we calculate peak isometric stress of the starling pectoralis to be 122 kPa. This is low in comparison to most measurements for striated muscle, which average closer to 200 kPa (Biewener *et al.* 1988*a*; Close, 1972; Wells, 1965). However, our estimate of fiber cross-sectional area probably overestimates the actual contractile myofibrillar area of the pectoralis by a considerable amount. The

starling pectoralis is composed exclusively of oxidative muscle fibers (Rosser and George, 1985), analogous to the fast twitch oxidative glycolytic or red intermediate fibers of mammals. Quantitative measurements of similar oxidative fibers in the pigeon show that mitochondrial volume density averages nearly 30 % of the whole fiber (James and Meek, 1979). Additionally, Conley *et al.* (1987) find for different-sized mammalian species that the number of capillaries per unit area of various muscles within these animals is well correlated with their mitochondrial volume density. Based on the measurements of Conley *et al.* (1987), a mitochondrial volume density of 30 % corresponds to roughly 10 % of a fiber's area being occupied by capillaries supplying oxygen to the mitochondria. Assuming that the starling pectoralis has similarly high mitochondrial and capillary volume densities to the pigeon pectoralis, the actual myofibrillar cross-sectional area of the pectoralis for the birds in this study is more likely to be only 112 mm^2, indicating a peak isometric stress of 204 kPa based on our *in situ* measurements of force.

Because the pectoralis is actively stretched during the upstroke and subsequently shortens during the downstoke, the comparison of peak muscle force measured during flight with that of maximal isometric force is not a valid index of muscle fiber recruitment levels (being 28 % of peak isometric force). When rapidly stretched, skeletal muscle can exert forces that may exceed peak isometric force by 50–75 % (Abbott and Aubert, 1952; Biewener *et al.* 1988*a*; Cavagna and Citterio, 1974; Harry *et al.* 1990; Katz, 1939), suggesting that a smaller motor unit pool would be needed to develop the observed force during the upstroke to decelerate the wing than under isometric conditions. However, the pectoralis develops maximal force a long time after being stretched as it shortens to pull the wing down (Fig. 6). Consequently, as it shortens (averaging 6.7 muscle fiber lengths s^{-1} during the downstroke under these flight conditions), considerably more than 28 % of the muscle's fibers would be needed to generate the observed force. Measurements of the muscle's force–velocity properties and direct measurements of fiber length change during flight are needed before fiber recruitment levels can be reliably evaluated in the context of measurements of muscle force.

Comparisons with other species

Based on fixed-wing steady-state aerodynamics, Pennycuick (1968) calculates the sustained power output for a pigeon (0.33 kg body mass) flying at a similar speed to be about 10 W. Given a combined pectoralis muscle mass of 0.060 kg in pigeons of this size (K. P. Dial and A. A. Biewener, in preparation), this indicates a mass-specific power output of 167 W kg^{-1} muscle, which is 1.6 times greater than that of the smaller starling. Indeed, because of its lower wing-beat frequency (5–6 Hz) at this speed, one would expect the pigeon to have a lower mass-specific power output than the starling, assuming equivalent muscle stress and shortening strain (Pennycuick and Rezende, 1984). Mass-specific mean power output of the starling pectoralis is also considerably below the maximum predicted for vertebrate striated muscle (250 W kg^{-1}; Weis-Fogh and Alexander, 1977). Torre-Bueno and Larochelle (1978) report a metabolic rate of 8.9 W for starlings during

steady level flight that changed very little over a range of flight speeds from 8 to 18 m s^{-1}. Combining their metabolic data with our calculation of mechanical power output yields an overall flight efficiency of 13 % for the starling at a speed near 13.7 m s^{-1}. This is comparable to that estimated for small running mammals and birds (Heglund *et al.* 1982) but is below estimates of the partial efficiencies (defined as the change in work rate/change in metabolic rate) of flying birds (19–30 %; Tucker, 1972; Bernstein *et al.* 1973) and bats (19–27 %; Thomas, 1975), based on calculations of mechanical power output using fixed-wing aerodynamic theory. The latter estimates are much closer to the maximum efficiency achieved by vertebrate striated muscle during a shortening contraction (20–25 %; Hill, 1939, 1964; Heglund and Cavagna, 1987).

The muscle stress that we calculate for the starling pectoralis based on total muscle fiber area is only 34 kPa during flight. However, if we account for 40 % of the fiber area being mitochondria and capillaries (see above), this yields a value of 57 kPa exerted by the myofilaments, which is slightly lower than that observed in the ankle extensor muscles of terrestrial mammals moving at their preferred speed (80 kPa, after correcting for estimated capillary and mitochondrial volume fractions; Perry *et al.* 1988). Because the birds were flown in a wind tunnel we could not determine their preferred flight speed, but earlier work indicates that starlings prefer to fly at a speed near 13.5 m s^{-1} (Torre-Bueno and Larochelle, 1978). The lower stress in the starling pectoralis may reflect, in part, the greater extent of shortening and positive work performed by this muscle during flight compared to the ankle extensors of terrestrial animals during steady locomotion. In addition, reduced fiber recruitment levels may also indicate a strategy for increased flight endurance or that force requirements during non-steady flight may be much greater than those during steady level flight. The much lower mean power output of the starling compared to the theoretical maximum for vertebrate striated muscle supports either of these possibilities. In addition to improvements of the flow conditions in future wind tunnel experiments, measurements of pectoralis force and mechanical power output over a range of flight speeds and flight conditions (take-off, ascent and descent) are needed for a better evaluation of the theoretical basis of previously developed aerodynamic models of flapping flight.

References

ABBOTT, B. C. AND AUBERT, X. M. (1952). The force exerted by active striated muscle during and after change in length. *J. Physiol., Lond.* 117, 77–86.

ALEXANDER, R., McN. (1977). Allometry of the limbs of antelopes (Bovidae). *J. Zool., Lond.* **183**, 125-146.

BERNSTEIN, M. H., THOMAS, S. P. AND SCHMIDT-NIELSEN, K. (1973). Power input during flight of the fish crow, *Corvus ossifragus. J. exp. Biol.* **58**, 401-410.

BIEWENER, A. A., BLICKHAN, R., PERRY, A. K., HEGLUND, N. C. AND TAYLOR, C. R. (1988a). Muscle forces during locomotion in kangaroo rats: force platform and tendon buckle measurements compared. *J. exp. Biol.* **137**, 191-205.

BIEWENER, A. A. AND TAYLOR, C. R. (1986). Bone strain: a determinant of gait and speed? *J. exp. Biol.* **123**, 383-400.

BIEWENER, A. A., THOMASON, J. AND LANYON, L. E. (1988b). Mechanics of locomotion and jumping in the horse (*Equus*): *in vivo* stress in the tibia and metatarsus. *J. Zool., Lond.* **214**, 547-565.

BROWN, R. J. H. (1963). The flight of birds. *Biol. Rev.* **38**, 460-489.

CARPENTER, R. E. (1985). Flight physiology of flying foxes, *Pteropus poliocephalus. J. exp. Biol.* **114**, 619-647.

CAVAGNA, G. A. AND CITTERIO, G. (1974). Effect of stretching on the elastic characteristics and the contractile component of frog striated muscle. *J. Physiol., Lond.* **239**, 1-14.

CLOSE, R. I. (1972). Dynamic properties of mammalian skeletal fibers. *Physiol. Rev.* **52**, 129-197.

CONLEY, K. E., KAYAR, S. R., ROSLER, K., HOPPELER, H., WEIBEL, E. R. AND TAYLOR, C. R. (1987). Adaptive variation in the mammalian respiratory system in relation to energetic demand. IV. Capillaries and their relationship to oxidative capacity. *Respir. Physiol.* **69**, 47-64.

DIAL, K. P., JENKINS, F. A., JR AND GOSLOW, G. E., JR (1991). The functional anatomy of the shoulder in the European starling (*Sturnus vulgaris*). *J. Morph.* **207**, 327-344.

ELLINGTON, C. P., MACHIN, K. E. AND CASEY, T. M. (1990). Oxygen consumption of bumblebees in forward flight. *Nature* **347**, 472-473.

GREENEWALT, C. H. (1975). The flight of birds. *Trans. Am. phil. Soc.* **65**, 1-67.

HARRY, J. D., WARD, A. W., HEGLUND, N. C., MORGAN, D. L. AND McMAHON, T. A. (1990). Cross-bridge cycling theories cannot explain high-speed lengthening behavior in muscle. *Biophys. J.* **57**, 201-208.

HEGLUND, N. C. AND CAVAGNA, G. A. (1987). Mechanical work, oxygen consumption and efficiency in isolated frog and rat striated muscle. *Am. J. Physiol.* **253**, C22-C29.

HEGLUND, N. C., FEDAK, M. A., TAYLOR, C. R. AND CAVAGNA, G. A. (1982). Energetics and mechanics of terrestrial locomotion. IV. Total mechanical energy changes as a function of speed and body size in birds and mammals. *J. exp. Biol.* **97**, 57-66.

HILL, A. V. (1939). The mechanical efficiency of frog's muscle. *Proc. R. Soc. B* **127**, 434-451.

HILL, A. V. (1964). The efficiency of mechanical power development during muscular shortening and its relation to load. *Proc. R. Soc. Lond. B* **159**, 319-324.

HUDSON, D. M. AND BERNSTEIN, M. H. (1983). Gas exchange and energy cost of flight in the white-necked raven, *Corvus cryptoleucus. J. exp. Biol.* **103**, 121-130.

JAMES, N. T. AND MEEK, G. A. (1979). Stereological analyses of the structure of mitochondria in pigeon skeletal muscle. *Cell Tissue Res.* **202**, 493-503.

JENKINS, F. A., DIAL, K. P. AND GOSLOW, G. E. (1988). A cineradiographic analysis of bird flight: the wishbone in starlings is a spring. *Science* **241**, 1495-1498.

KATZ, B. (1939). The relation between force and speed in muscular contraction. *J. Physiol., Lond.* **96**, 45-64.

KOKSHAYSKY, N. V. (1979). Tracing the wake of a flying bird. *Nature* **279**, 146-148.

LAKES, R. S., KATZ, J. L. AND STERNSTEIN, S. S. (1979). Viscoelastic properties of wet cortical bone. I. Torsional and biaxial studies. *J. Biomech.* **12**, 657-678.

LIGHTHILL, J. (1977). Introduction to the scaling of aerial locomotion. In *Scale Effects in Animal Locomotion* (ed. T. J. Pedley), pp. 365-404. London: Academic Press.

PENNYCUICK, C. J. (1968). Power requirements for horizontal flight in the pigeon *Columba livia. J. exp. Biol.* **49**, 527-555.

PENNYCUICK, C. J. (1989). *Bird Flight Performance. A Practical Calculation Manual.* Oxford: Oxford University Press.

PENNYCUICK, C. J. AND REZENDE, M. A. (1984). The specific power output of aerobic muscle, related to the power density of mitochondria. *J. exp. Biol.* **108**, 377-392.

PERRY, A. K., BLICKHAN, R., BIEWENER, A. A., HEGLUND, N. C. AND TAYLOR, C. R. (1988). Preferred speeds in terrestrial vertebrates: are they equivalent? *J. exp. Biol.* **137**, 207–220.

RAYNER, J. M. V. (1979). A new approach to animal flight mechanics. *J. exp. Biol.* **80**, 17–54.

RAYNER, J. M. V., JONES, G. AND THOMAS, A. (1986). Vortex flow visualizations reveal change in upstroke function with flight speed in bats. *Nature* **321**, 162–164.

ROSSER, B. W. C. AND GEORGE, J. C. (1986). The avian pectoralis: histochemical characterization and distribution of muscle fiber types. *Can. J. Zool.* **64**, 1174–1185.

ROTHE, H.-J. AND NACHTIGALL, W. (1987). Pigeon flight in a wind tunnel. *J. comp. Physiol.* B **157**, 91–98.

RUBIN, C. T. AND LANYON, L. E. (1982). Limb mechanics as a function of speed and gait: a study of functional strains in the radius and tibia of horse and dog. *J. exp. Biol.* **101**, 187–211.

SPEDDING, G. R. (1987). The wake of a kestrel (*Falco tinnuculus*) in flapping flight. *J. exp. Biol.* **127**, 59–78.

SPEDDING, G. R., RAYNER, J. M. V. AND PENNYCUICK, C. J. (1984). Momentum and energy in the wake of a pigeon (*Columba livia*) in slow flight. *J. exp. Biol.* **111**, 81–102.

THOMAS, S. P. (1975). Metabolism during flight in two species of bats, *Phyllostomus hastatus* and *Pteropus gouldii*. *J. exp. Biol.* **63**, 273–293.

TORRE-BUENO, J. R. AND LAROCHELLE, J. (1978). The metabolic cost of flight in unrestrained birds. *J. exp. Biol.* **75**, 223–229.

TUCKER, V. A. (1968). Respiratory exchange and evaporative water loss in the flying budgerigar. *J. exp. Biol.* **48**, 67–87.

TUCKER, V. A. (1972). Metabolism during flight in the laughing gull, *Larus atricilla*. *Am. J. Physiol.* **222**, 237–245.

TUCKER, V. A. AND PARROTT, G. C. (1970). Aerodynamics of gliding flight in a falcon and other birds. *J. exp. Biol.* **52**, 345–367.

WEIS-FOGH, T. (1972). The energetics of hovering flight in hummingbirds and *Drosophila*. *J. exp. Biol.* **56**, 79–104.

WEIS-FOGH, T. AND ALEXANDER, R. McN. (1977). The sustained power output from striated muscle. In *Scale Effects in Animal Locomotion* (ed. T. J. Pedley), pp. 511–525. London: Academic Press.

WELLS, J. B. (1965). Comparisons of mechanical properties between slow and fast mammalian muscles. *J. Physiol., Lond.* **178**, 252–269.